Supporting Information

Morphology and electronic modulation of composite nanosheets for electrocatalytic oxygen evolution through partial and in-situ transformation of NiFe-LDH

Xiaodong Yang[a,#], Zihan Zhao[a,#], Qi Shen[a,*], Chen Xu[a], Chuanxin Shi[a], Wenwen Cao[a], Yiqiang Sun[a,b,c,*], Bo Xu[a,*]

---

a School of Chemistry and Chemical Engineering, University of Jinan, Shandong, Jinan, 250022, China
b School of Materials Science And Engineering, University of Jinan, Shandong, Jinan 250022, China
c Foshan (Southern China) Institute for New Materials, Foshan 528200, Guangdong, China

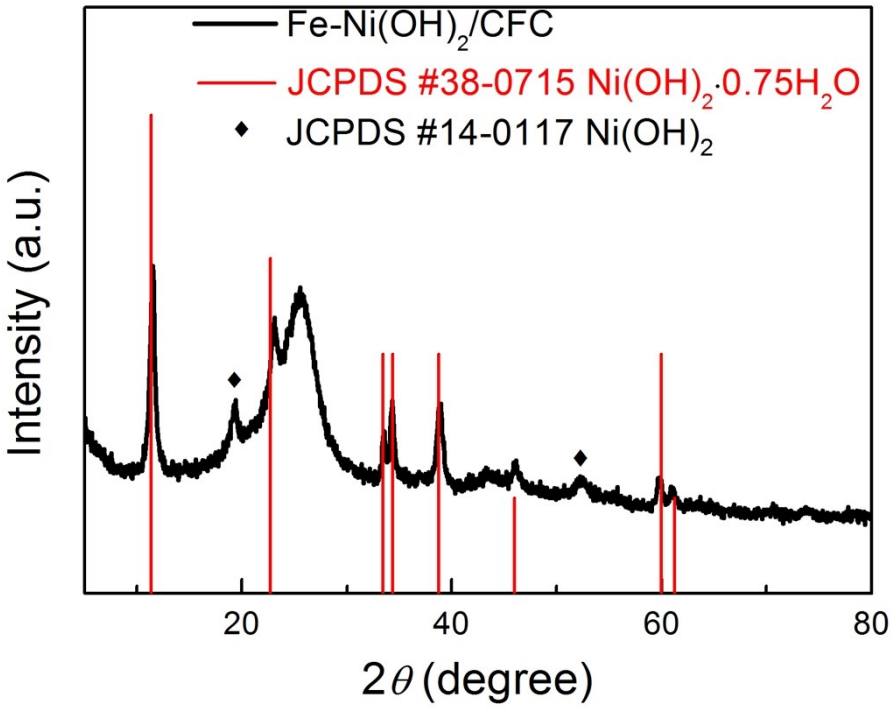

Figure S1. XRD diffraction pattern of Fe-Ni(OH)$_2$/CFC and standard Ni(OH)$_2$·0.75H$_2$O characteristic peak (♦ represents the characteristic peak of Ni(OH)$_2$).

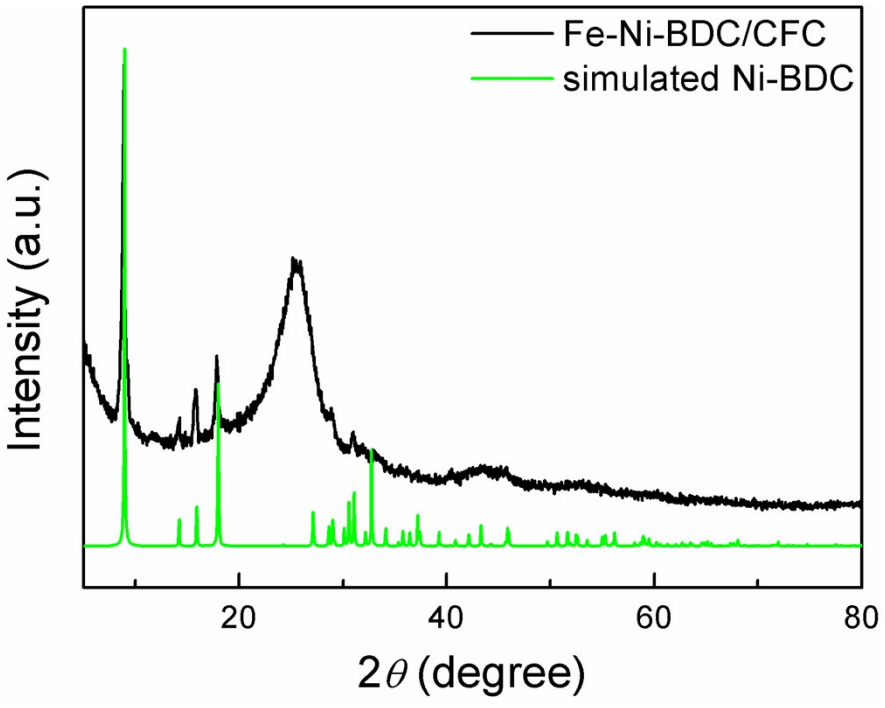

Figure S2. XRD diffraction pattern of Fe-Ni-BDC/CFC with standard simulated

curve.

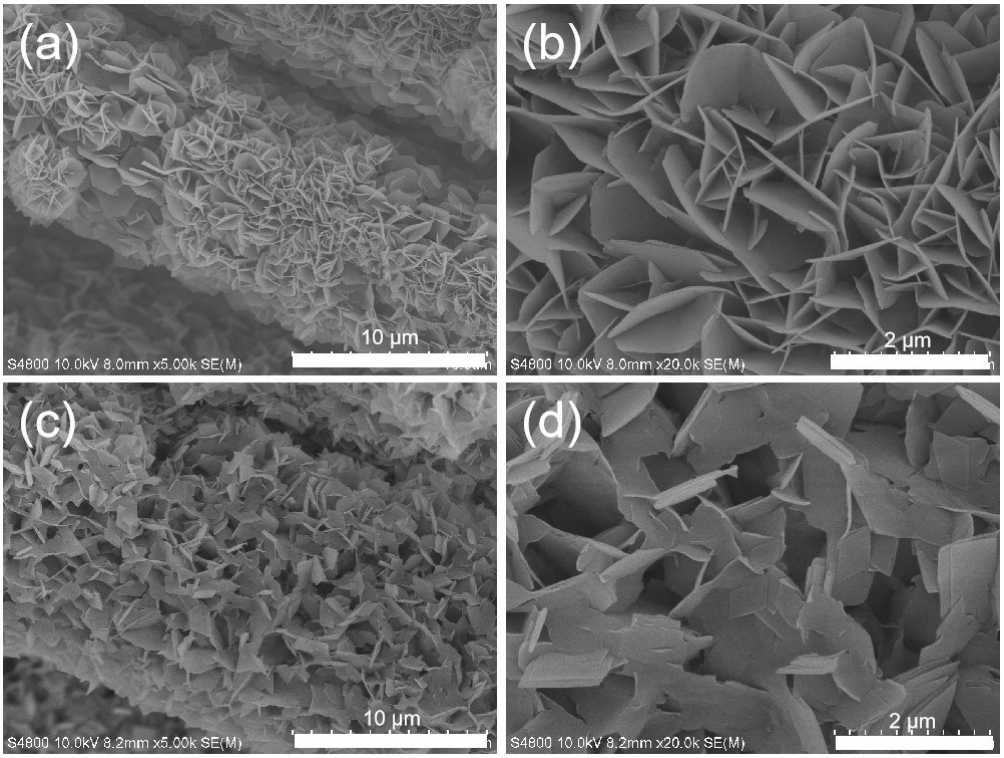

Figure S3. (a, b) SEM images with different magnifications of Fe-Ni$(OH)_2$/CFC with different magnifications; (c, d) SEM images with different magnifications of Fe-Ni-BDC/CFC with different magnifications.

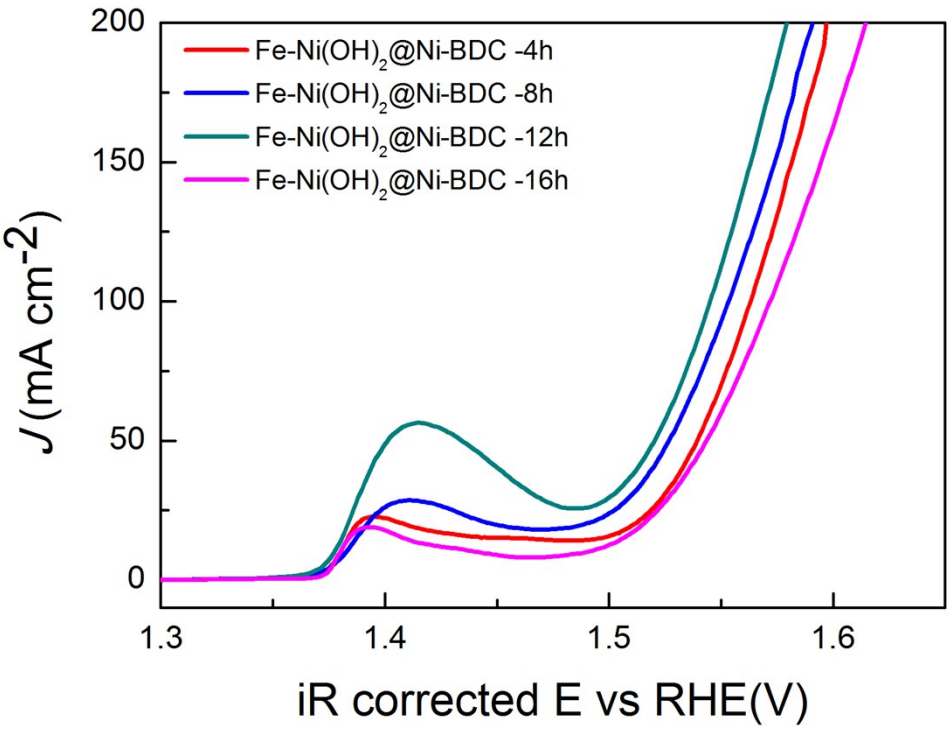

Figure S4. LSV curves of Fe-Ni(OH)$_2$@Ni-BDC/CFC-X (X = 4, 8, 12, 16).

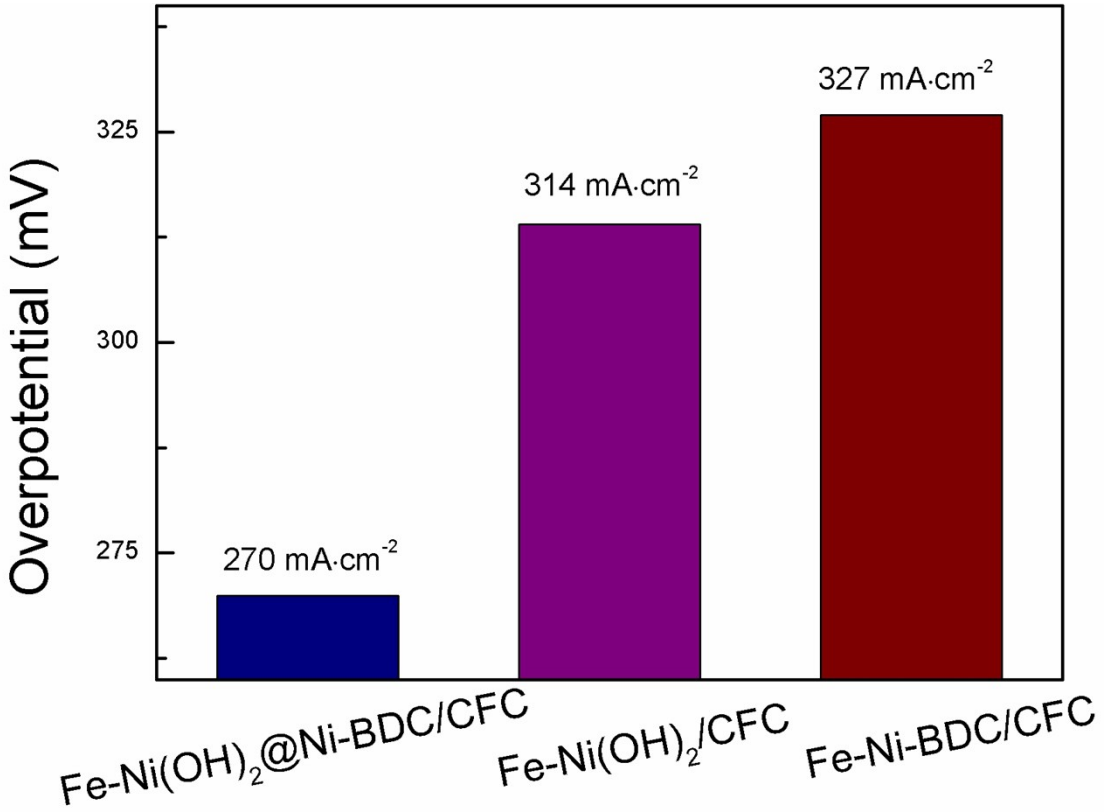

Figure S5. Overpotential of Fe-Ni(OH)$_2$@Ni-BDC/CFC, Fe-Ni(OH)$_2$/CFC and Fe-Ni-BDC/CFC at 30 mA cm^{-2} Vs Ag/AgCl.

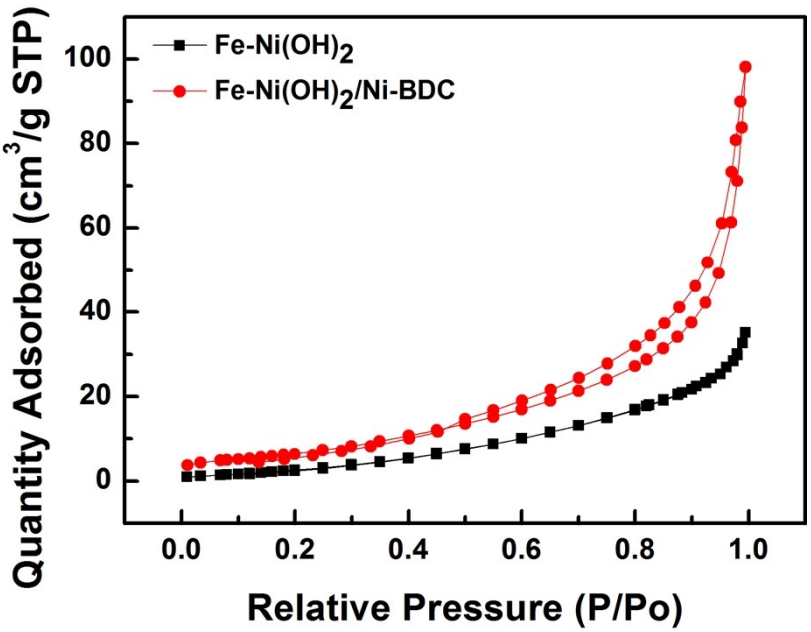

Figure S6. The nitrogen adsorption-desorption isotherm Fe-Ni(OH)$_2$ and Fe-Ni(OH)$_2$@Ni-BDC/CFC.

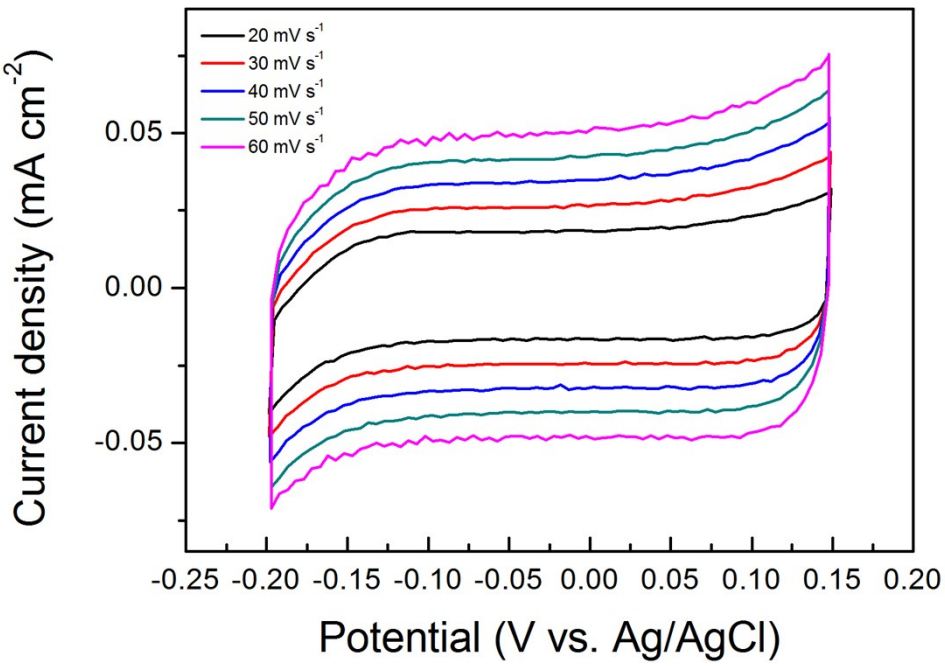

Figure S7. Cyclic voltammetry curves of Fe-Ni$(OH)_2$/CFC at a scan rate of 20 to 60 mV/sv for determining their C_{dl} data.

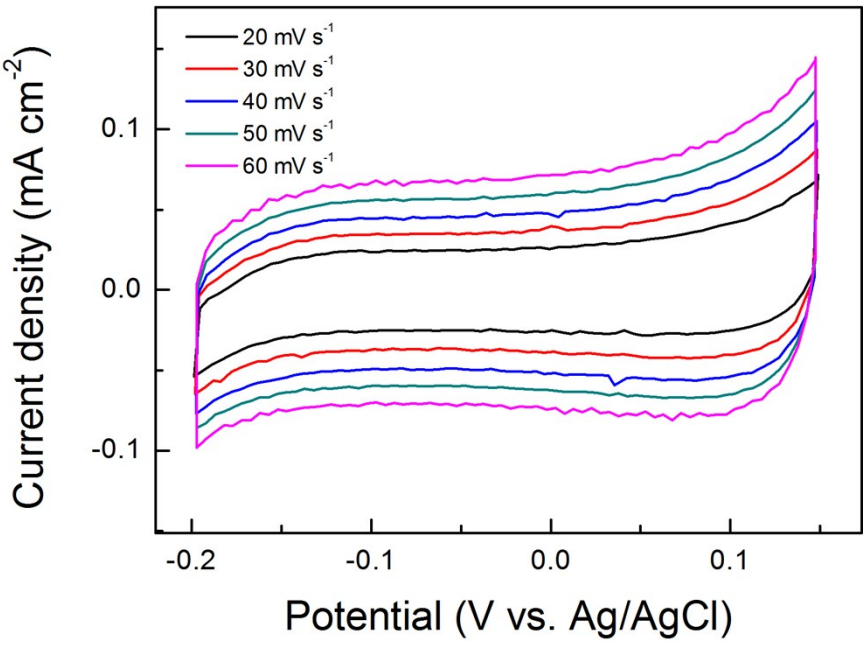

Figure S8. Cyclic voltammetry curves of Fe-Ni(OH)$_2$@Ni-BDC/CFC at a scan rate of 20 to 60 mV s^{-1} for determining their C_{dl} data.

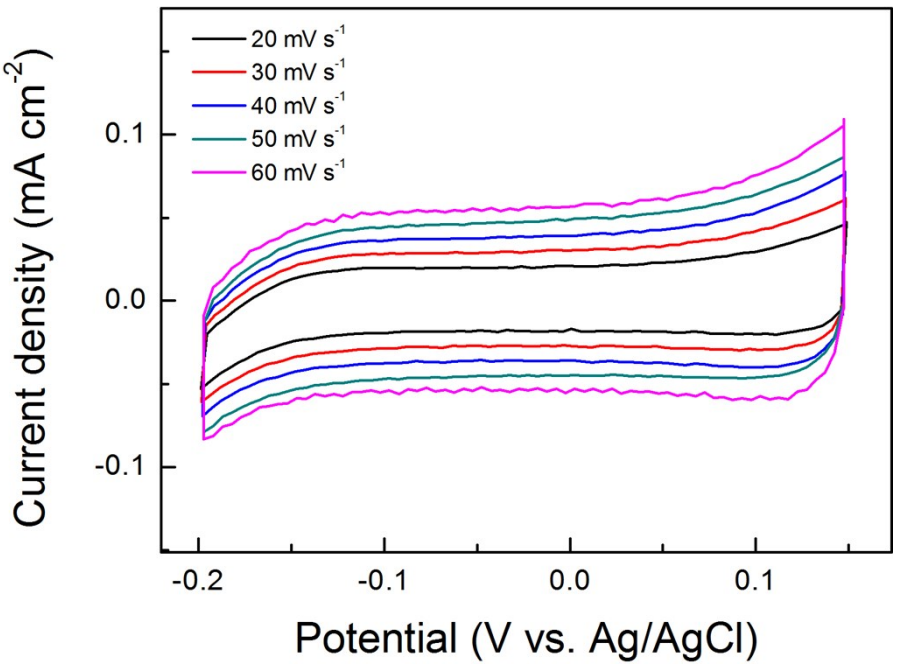

Figure S9. Cyclic voltammetry curves of Fe-Ni-BDC/CFC at a scan rate of 20 to 60 mV s^{-1} for determining their C_{dl} data.

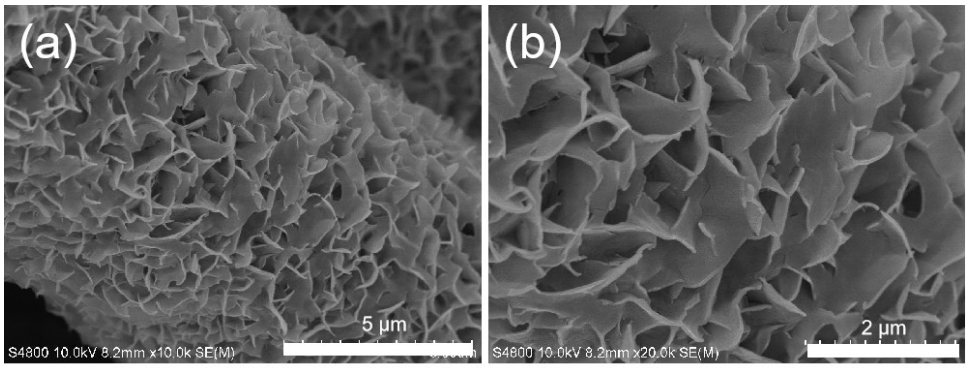

Figure S10. (a, b) SEM images with different magnifications of Fe-Ni(OH)$_2$@Ni-BDC/CFC after electrocatalytic stability test.

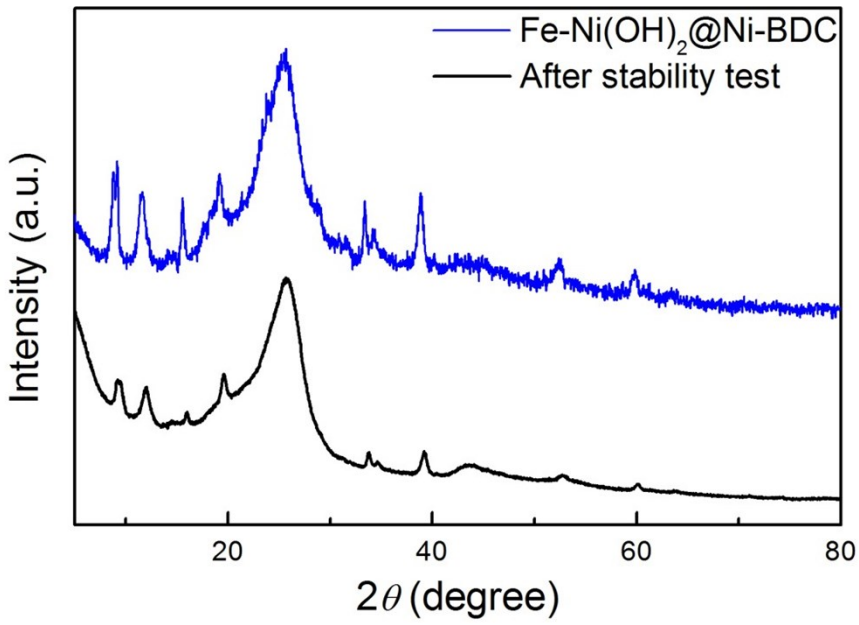

Figure S11. XRD diffraction pattern of Fe-Ni(OH)$_2$@Ni-BDC/CFC before and after electrocatalytic stability test.

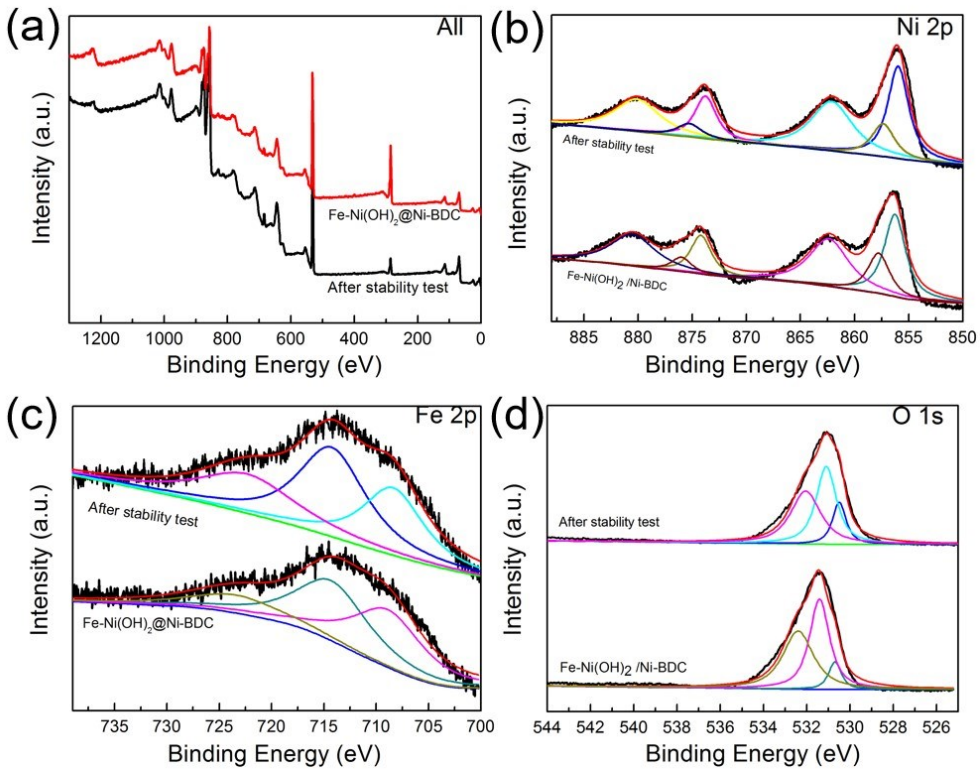

Figure S12. (a) XPS survey spectra for Fe-Ni(OH)$_2$@Ni-BDC/CFC after stability test; (b) The Ni 2p XPS spectra for Fe-Ni(OH)$_2$@Ni-BDC/CFC after stability test; (c) The Fe 2p XPS spectra for Fe-Ni(OH)$_2$@Ni-BDC/CFC after stability test; (d) The O 1s XPS spectra for Fe-Ni(OH)$_2$@Ni-BDC/CFC after stability test.

Table S1. Comparison of the OER performance of Fe-Ni(OH)$_2$@Ni-BDC/CFC with some NiFe based catalysts.

Catalyst	Overpotential/mV	Electrolyte	Reference
Fe-Ni(OH)$_2$@Ni-BDC/CFC	270 @ 30 mA/cm^2	1.0 M KOH	This work
NiCdFe	290 @ 10 mA/cm^2	1.0 M KOH	Appl Catal B-Environ 2018, 225, 1
FeOOH/NiFe LDHs@CCH NAs-NF	330 @ 100 mA/cm^2	1.0 M KOH	J. Mater. Chem. A, 2018, 6, 3397
Ni-Fe-Co alloy nanocones	310 @ 10 mA/cm^2	1.0 M KOH	J.Colloid.Interf.Sci., 2019,547,407
NiFe/C	300 @ 10 mA/cm^2	1.0 M KOH	ACS Catal., 2016,6,4477
NiCoFe-LDH	280 @ 10 mA/cm^2	1.0 M KOH	Electrochim Acta., 2016,8,5327
(Ni, Fe)S$_2$@MoS$_2$	270 @ 10 mA/cm^2	1.0 M KOH	Appl Catal B-Environ, 2019, 247, 107
NiFe hydroxysulfide	286 @ 10 mA/cm^2	1.0 M KOH	Energy Environ. Sci, 2020,13, 1711
S-doped NiFe-LDH	300 @ 100 mA/cm^2	1.0 M KOH	Energy Environ. Sci, 2020,13, 3439